16th World Conference on Earthquake, 16WCEE 2017

Santiago Chile, January 9th to 13th 2017

Paper N° 2705

Registration Code: S-I1464667166

DESIGN AND VALIDATION OF STEEL SELF-CENTERING CONCENTRICALLY-BRACED FRAMES

N.B. Chancellor[1], R. Sause[2], J.M. Ricles[3]

[1] *Senior Design Engineer, Leslie E. Robertson Associates, brent.chancellor1@gmail.com*
[2] *Joseph T. Stuart Professor, Lehigh University, rs0c@lehigh.edu*
[3] *Bruce G. Johnston Professor, Lehigh University, jmr5@lehigh.edu*

Abstract

Steel self-centering concentrically-braced frames (SC-CBFs), also known as rocking braced frames, are a relatively new seismic lateral force resisting system. Exceptional seismic performance of SC-CBFs has been demonstrated in a number of laboratory tests. There is not, however, a well-established design procedure for SC-CBFs available for practicing design engineers who wish to incorporate SC-CBFs into their structures. This paper presents a design procedure for SC-CBFs based on conventional response-spectrum analysis, modified to account for significant higher mode effects. This design procedure for SC-CBFs predicts story shears and overturning moments under the median design basis earthquake so that peak member force demands are determined that have a small probability of exceedance. Results of extensive analytical studies on SC-CBFs ranging in height from 4 to 12 stories designed with this procedure are presented to validate the SC-CBF design procedure.

Keywords: self-centering; modal combination; higher mode effects; design procedure

1. Introduction

Steel Self-Centering Concentrically-Braced Frames (SC-CBFs), also known as rocking braced frames, are a relatively new seismic lateral force resisting system. SC-CBFs reduce or eliminate structural damage under the Design Basis Earthquake (DBE) by allowing lateral drift to occur in the braced frame largely as a rigid body mode (rocking) [1, 2]. Seismic energy is dissipated through reusable or replaceable energy dissipation elements. Damage to the braces and other members is not a significant energy dissipation mechanism in SC-CBFs. A restoring force acts on the braced frame to self-center the braced frame after ground shaking has stopped, leaving little or no residual drift. This restoring force usually is provided by vertical post-tensioning (PT) steel bars spanning from the foundation to the top of the braced frame, gravity loads, or a combination of both [1, 2, 3]. Figure 1 schematically shows the rocking behavior and elements of an SC-CBF. Schematic details of floor diaphragm connections and foundation shear connections are found in [4, 5, 6].

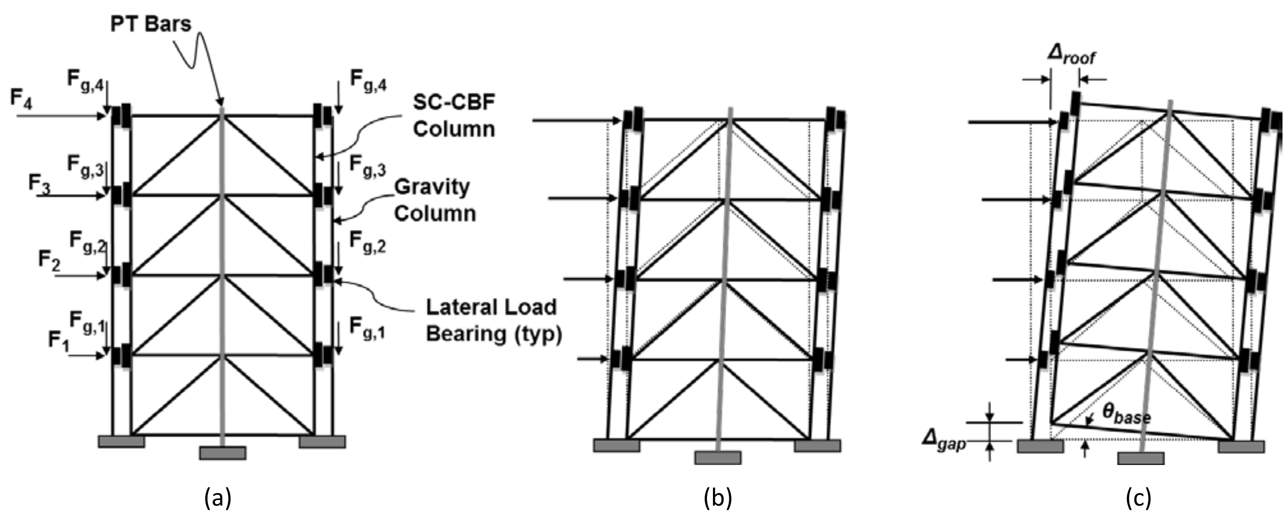

Fig. 1 – Lateral load behavior of SC-CBF: (a) layout of typical SC-CBF with gravity and lateral forces; (b) elastic response of SC-CBF frame before SC-CBF “tension” column decompresses and lifts up; (c) rigid body rocking of frame on foundation [7].

The SC-CBF has 4 fundamental limit states: decompression/uplift of the “tension” column, yielding of the PT steel, yielding of frame member elements, and failure of frame elements (buckling, fracture). These limit states are shown schematically on an overturning moment-drift plot in Figure 2(a). In a well-designed SC-CBF, the limit states will occur in the order shown, as this limits the damage and residual drift of the braced frame. The characteristics of the SC-CBFs, such as amount and initial prestress force level of PT steel, amount of supplemental energy dissipation, and strength and ductility of the members of the braced frame can all be tuned to eliminate damage and residual drift of the SC-CBF without excessive lateral drift.

The hysteretic behavior of the SC-CBF system is characterized by flag shaped hysteresis loops [1]. Energy dissipation is supplied by replaceable or reusable elements such as hysteretic elements or friction bearings. As shown in Figure 2(b), the overturning moment-drift history passes through the origin on each cycle, resulting in no residual drift. This characteristic is unique to self-centering systems.

Exceptional seismic performance of SC-CBFs has been demonstrated in a number of laboratory tests showing that damage free performance is possible under the DBE without excessive lateral drift and no residual drift [2,6]. These tests also showed the presence of significant higher mode response [2]. The remainder of this paper presents and validates a design procedure for SC-CBFs based on conventional response-spectrum analysis, modified to account for significant higher mode effects.

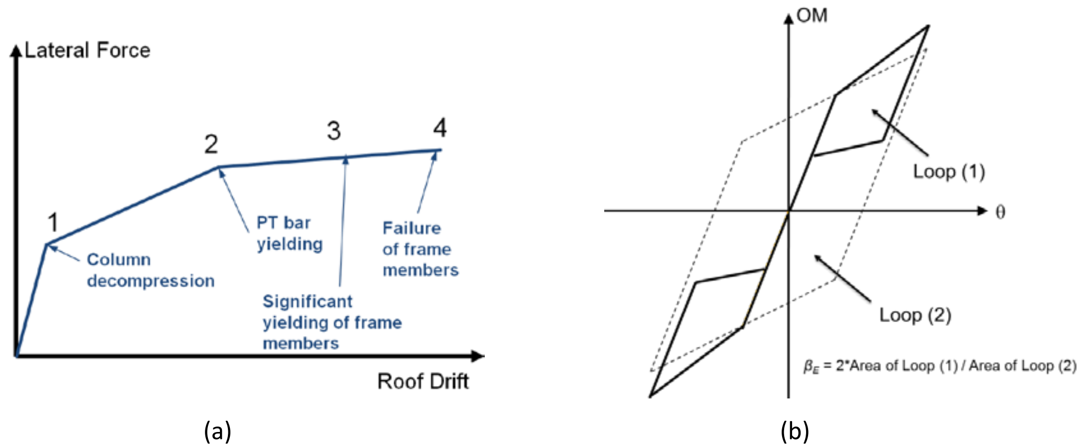

Fig. 2 – (a) Limit states of SC-CBF; (b) hysteretic behavior of SC-CBF [7]

2. Design Procedure for SC-CBFs

The design procedure for SC-CBFs should have the following characteristics:

- Be as simple as possible so that it can be easily understood and applied by practicing engineers,
- Estimate member forces and drifts with a reasonable level of accuracy for structures across a broad range of aspect ratios (i.e., frame height-to-width),
- Properly account for key SC-CBF behavior, such as significant higher mode response,
- Result in designs with low probabilities of damage to SC-CBF members,
- Result in designs that do not have excessive drift,
- Result in designs that have little to no residual drift.

The SC-CBF design procedure presented and validated below incorporates all these characteristics. However the drift portion of this design procedure is not presented or validated in this paper. Instead the reader should refer to [8].

The design procedure proposed in this paper to determine member force design demands is based on a conventional modal response spectrum analysis (RSA) in order to be simple and familiar to practicing engineers. In conventional modal RSA, an elastic design spectrum representing the building site seismicity at a specific hazard level (e.g., spectral acceleration with a 10% probability of exceedance (POE) in 50 years) is uniformly reduced across all periods by a system-based response modification coefficient (R) to account for nonlinear system behavior. This is shown schematically in Figure 3.

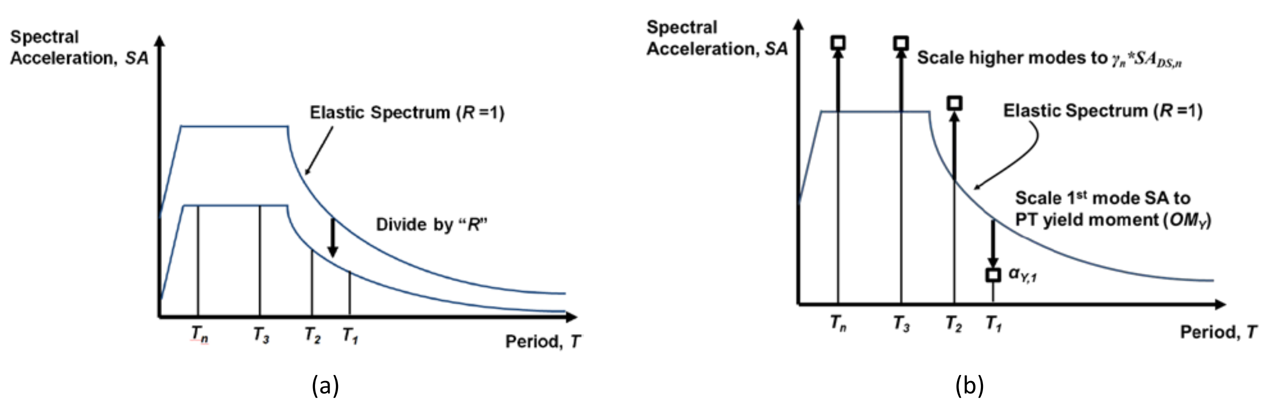

Fig. 3 – (a) Conventional RSA design spectral accelerations; (b) spectral accelerations for design of SC-CBFs

Elastic modal properties are calculated and the peak modal force demands on the structure are determined using this reduced design spectrum. The peak overall structural response is estimated by combining the peak modal responses using a modal combination procedure such as the square root of the sum of the squares (SRSS) or the complete quadratic combination (CQC). The SRSS rule assumes that there is no correlation between the peak modal responses of two different modes at the time of peak response of the structure while the CQC modal combination procedure accounts for correlation between peak modal responses at the time of peak structural response. Modal correlation coefficients proposed by Der Kiureghian [9] are widely accepted and used by practicing engineers. Der Kiureghian's modal correlation coefficients vary from 0 to 1 and are always positive.

The proposed SC-CBF design procedure uses the method of modal RSA, modified to account for the behavior of rocking structures. Rocking structures are characterized by a base flexural mechanism. This mechanism is primarily a first mode mechanism and largely limits the peak response of the first mode. Higher modes are not limited and generally respond elastically or are amplified by the rocking action [2, 8]. Therefore, uniformly reducing the design spectrum is not appropriate for SC-CBFs. Instead the first mode spectral acceleration is scaled so the first base mode overturning moment is equal to the base overturning moment at yield of the PT steel. This scaling method allows a high probability (up to 50%) that the PT steel will yield under the DBE. However, since ductile steel bars (e.g., Dywidag threadbars) are used, and can be easily restressed after the earthquake if they have yielded, then this limit state is not considered to be significant structural damage.

The higher mode spectral accelerations are not reduced, rather they are amplified using modal load factors so that there is a small probability of exceeding the member design demand (5%-10% POE) under the DBE. The adjustment to the first mode and higher modes spectral acceleration(s) in the SC-CBF design procedure is shown in Figure 3(b). A modal load factor, γ_1, is applied to the first mode because it has been shown that the first mode base overturning moment can exceed the base overturning moment at yield of the PT steel [8]. This phenomenon is possible due to the presence of higher modes in the base overturning moment response [8]. The modal load factors are determined using the following equations:

$$\gamma_1 = \begin{Bmatrix} 1.15 & h_{SC-CBF} \le 16\ m \\ 0.036 \cdot \left(\dfrac{h_{SC-CBF}}{m} \right) + 0.58 & 16\ m < h_{SC-CBF} < 39\ m \\ 2.0 & h_{SC-CBF} > 39\ m \end{Bmatrix} \tag{1}$$

$$\gamma_n = 1.6 \ \ when\ n \ne 1 \tag{2}$$

In Eq.(1) $h_{SC\text{-}CBF}$ is the height of the SC-CBF in meters. Note that the modal load factors are used to determine member force design demands which have a low probability of exceedance. Chancellor [8] proposes other (reduced) modal load factors when a higher probability of member damage is acceptable to the designer.

Chancellor [8] showed that peak modal responses for SC-CBFs can occur almost at the same time for multiple modes, indicating significant modal correlation. It was also shown that this correlation can be negative. Therefore, the SRSS procedure is not appropriate for SC-CBFs and Der Kiureghian's [9] modal correlation coefficients with the CQC procedure will not adequately estimate peak member force demands in SC-CBFs. Additionally, Chancellor [8] showed that the correlation between peak modal responses at the time of peak member force demand is different based on the member type (e.g., brace or column) and location in the structure. To adequately estimate the peak member force demands in SC-CBFs a modification is proposed to the conventional CQC and SRSS procedures.

Once the scaled modal member force demands are determined using the modal load factors, γ_n, the modes are combined using the modal combination procedure described below. The modal combination procedure proposed for the design of SC-CBFs, denoted as 2CQC, is similar to the CQC procedure, but the modal combination is carried out twice. A different set of cross-modal correlation coefficients is used in each modal combination. The maximum result of the two modal combinations is then taken as the design demand. The 2CQC procedure for calculating the design demand, r_{design}, is:

$$r_{design} = \max\left(\left(\sum_{i=1}^{N}\sum_{n=1}^{N}\rho_{1in}\cdot r_{i0}\cdot r_{n0}\right)^{\frac{1}{2}}, \left(\sum_{i=1}^{N}\sum_{n=1}^{N}\rho_{2in}\cdot r_{i0}\cdot r_{n0}\right)^{\frac{1}{2}}\right) \tag{3}$$

where,

ri_0 = the peak response quantity in mode i

r_{n0} = the peak response quantity in mode n

ρ_{1in} = 1st set of cross-modal correlation coefficients for modes i and n

ρ_{2in} = 2nd set of cross-modal correlation coefficients for modes i and n

Since Der Kiureghian's [9] cross-modal correlation coefficients will neither adequately account for the high correlation between modes at time of peak member response nor for the variation in correlation based on the location in the structure, alternative cross-modal correlation coefficients were studied [8]. Newly proposed coefficients include:

$$\rho_{in} = \left\{\begin{array}{cc} 1.0 & if\ i = n \\ -0.75 & if\ i = 1\ and\ n = 2\ or\ if\ i = 2\ and\ n = 1 \\ -0.75 & if\ i = 1\ and\ n = 3\ or\ if\ i = 3\ and\ n = 1 \\ 0.75 & if\ i = 2\ and\ n = 3\ or\ if\ i = 3\ and\ n = 2 \\ 0 & otherwise \end{array}\right\} \tag{4}$$

$$\rho_{in} = \left\{\begin{array}{ll} 1.0 & if\ i = n \\ 0.25 & if\ i \neq n \end{array}\right\} \tag{5}$$

$$\rho_{in} = \left\{\begin{array}{ll} 1.0 & if\ i = n \\ 0.0 & if\ i \neq n \end{array}\right\} \tag{6}$$

The cross-modal correlation coefficients in Eq. 4 account for the significant correlation that occurs between the first few modes and are important for predicting peak member force demands in over the height of the SC-CBF, particularly in the middle 2/3 of the height of the structure. The cross-modal correlation coefficients in Eq. 5 were proposed by Roke et al. [2] for the design of SC-CBFs using the conventional CQC modal combination procedure, but do not adequately estimate member force demands for SC-CBFs across a range of heights. However, the cross modal correlation coefficients in Eq. 5 are useful for capturing some of the higher mode effects on member force demands near the base of the SC-CBF. The cross-modal correlation coefficients in Eq. 6 correspond to the SRSS procedure.

Based on the studies by Chancellor [8] on SC-CBFs ranging from 4-stories to 18-stories in height, the cross-modal correlation coefficients in Eq. 4 (ρ_{1in}) and Eq. 5 (ρ_{2in}) were selected for use in the 2CQC procedure. These are the coefficients that are used for the design of the SC-CBFs in this paper.

3. Validation of SC-CBF Design Procedure

To demonstrate and validate the proposed SC-CBF design procedure, archetype SC-CBF structures of 4, 6, 9, and 12-stories are studied.

3.1 Archetype SC-CBF Designs

A schematic of the floor plan and elevation layouts for the archetype SC-CBFs structures are shown in Figure 4. The structures are symmetric in two directions with eight SC-CBFs distributed around the perimeter. This symmetry requires only a single SC-CBF for each structure to be designed.

The braces of the archetype SC-CBFs are arranged in an x-braced configuration. A gravity column is located adjacent to each SC-CBF column to separate the lateral movement of the floor system from the vertical movement of the SC-CBF during rocking. Lateral load bearings with friction transfer lateral loads from the floor diaphragm to the SC-CBF and provide a source of energy dissipation. High strength, high ductility post-tensioning (PT) bars run vertically over the height of the SC-CBF at mid-bay. A vertical distribution strut, shown in Figure 4(b), is located at the center of the bay in the top one or two stories to distribute the large concentrated force from the PT bars to the diagonal braces. A horizontal base strut is located at the bottom of the SC-CBF between the SC-CBF columns to transfer the base shear from the uplifted column to the column in contact with the foundation.

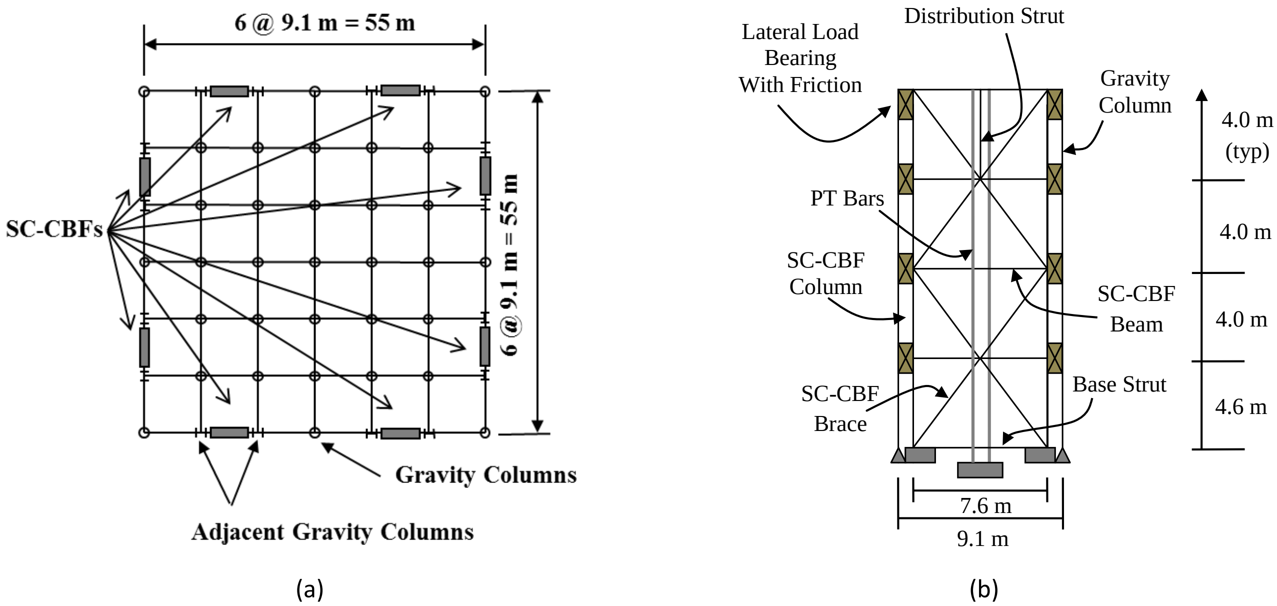

Fig. 4 – (a) Floor plan of archetype SC-CBFs; (b) elevation of archetype SC-CBF [7]

The floor dead load including self-weight and superimposed dead load is 4.2 kN/m^2. The roof dead load is 2.9 kN/m^2. The floor live load for gravity design is 3.1 kN/m^2. The roof live load is 0.96 kN/m^2. The live load included in the seismic mass (to account for partitions) is 0.72 kN/m^2 for the floors and 0 kN/m^2 for the roof.

All of the SC-CBF members were designed using wide-flange shapes that meet the seismic compactness requirements of ANSI/AISC 341-05 [10]. The specified yield strength of the steel for the SC-CBF and CBF members was 0.35 kN/mm^2 and the modulus of elasticity was 200 kN/mm^2. The yield strength for the PT bars for the SC-CBF was assumed to be 0.83 kN/mm^2 and the modulus of elasticity was assumed to be 205 kN/mm^2.

The seismic design category for the SC-CBF and CBF was Category D. The short period spectral acceleration used in design (S_S) was 1.5g and the 1 sec period spectral acceleration used in design (S_1) was 0.6g. The site class was assumed to be Site Class D.

Table 1 lists important parameters for each archetype SC-CBF design. The aspect ratio, as noted previously, is the height of the archetype SC-CBF divided by the width of the SC-CBF. T_1 is the first mode period of the SC-CBF calculated using a fixed base linear numerical model. θ_{DBE} is the predicted roof drift under the DBE and is limited to approximately 1.5% radians to control nonstructural damage. β_E is the energy dissipation ratio, which is the ratio of the area of idealized SC-CBF hysteresis loops to an equivalent bilinear elastic plastic system, see Figure 2(b). β_{SC} is a measure of the self-centering capability of the archetype SC-CBF and must be less than 0.50 to ensure self-centering behavior. In the design of SC-CBFs, a system specific response modification coefficient, R, such as those shown in in ASCE 7-10 [11] is not used. However, a response factor similar to R is calculated to show how much reduction in overturning moment demand the SC-CBF system provides relative to an elastic, fixed-base structure. This response factor, denoted R_A, is calculated as follows:

$$R_A = \frac{OM_{elastic}}{OM_D} \tag{7}$$

$OM_{elastic}$ is the base overturning moment calculated using the equivalent lateral forces from ASCE 7-10 [11] with R=1 and OM_D is the overturning moment when the SC-CBF uplifts and rocking begins.

$OM_{elastic}$ and OM_D are given in Table 2 for each archetype SC-CBF. The base overturning moment at yield of the PT steel (OM_Y) and the peak overturning moment predicted for the design basis earthquake (OM_{DBE}), which is based on estimated drift are also shown in Table 2. The area of PT steel and initial prestress ratio (initial prestress force/yield force) is summarized in Table 2.

Table 1 – Summary of design parameters for archetype SC-CBFs

Archetype	Aspect Ratio (height/width)	T_1 (sec)	θ_{DBE} (% rad)	β_E	β_{SC}	R_A	SC-CBF Weight (kN)
4-story	2.16	0.42	1.02	0.58	0.36	7.52	240
6-story	3.20	0.65	1.36	0.35	0.24	10.7	460
9-story	4.76	1.02	1.39	0.20	0.16	9.66	970
12-story	6.32	1.58	1.42	0.14	0.12	7.95	1540

Table 2 – Summary of additional design parameters for archetype SC-CBFs

Archetype	Area of PT Steel (cm^2)	Initial Prestress Ratio (% of Yield Force)	OM_D (MN-m)	OM_Y (MN-m)	$OM_{elastic}$ (MN-m)	OM_{DBE} (MN-m)
4-story	96.8	0.40	20.7	49.5	155.7	47.2
6-story	143	0.47	30.5	62.2	326.8	60.4
9-story	201	0.60	50.4	81.0	487.2	76.2
12-story	305	0.75	89.7	117.3	713.1	116.2

Figure 5 shows the wide flange shapes selected for each archetype SC-CBF as well as the ratio of the design demand to the capacity of the section (*DCR*). The DCR of most of the braces and columns is between 0.90 and 1.0. The DCR of some columns for the 12-story SC-CBF exceed 1.0, even with the largest section available in AISC [12] beam tables (W14x730). Since the columns are modeled as elastic in the time-history analyses (see Section 3.2) and the validation of the design procedure involves comparing calculated design demands with peak values from the time-history analyses, a decision was made to use the largest available section for these studies instead of designing built-up plate sections.

3.2 Modeling of Archetype SC-CBFs

Nonlinear numerical models of the archetype SC-CBFs for the time-history analyses were created in OpenSees, an open source nonlinear dynamic analysis software package [13]. The numerical model is a two dimensional (planar) model and is shown schematically in Figure 6.

The expected sources of nonlinear behavior in the SC-CBF are rocking and yielding of the PT steel. It is not expected that there will be significant nonlinearity in the SC-CBF members. Therefore, the SC-CBF members are modeled using elastic beam-column elements. The peak member force demand from the analyses will be compared with the member force design demand to evaluate this assumption.

The lateral load bearings are modeled using a friction-contact-gap element. The friction-contact-gap element models friction behavior using a Mohr-Coulomb friction model, modified to account for the contact and friction stiffness. A small, initial gap in the lateral load bearings is modeled.

The post-tensioning (PT) steel bars are modeled by a beam-column element with section and material properties such that the total area and axial yield force matches the design values. The PT bar material model is bilinear elastic-plastic with yield strength of 0.83 kN/mm^2 and a 2% post-yield slope. The PT bars are anchored at a node located at the center of the SC-CBF at the roof level and at a node 0.91 m below the base level. The 0.91 m of PT bar length below the base level represents the additional free length of PT bar in the foundation anchorage. At the node where the PT steel is anchored there is a zero-length element. The zero-length element is used to modify the PT steel model so that the PT steel carries only tension loads.

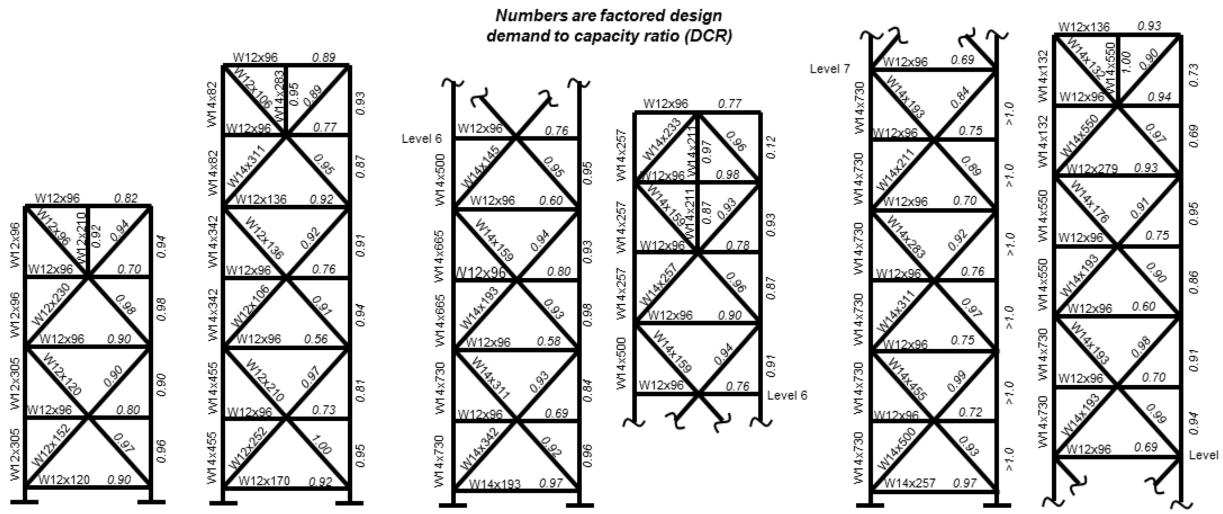

(a) (b) (c) (d)

Fig. 5 – Archetype SC-CBF designs: (a) 4-story, (b) 6-story, (c) 9-story, (d) 12-story

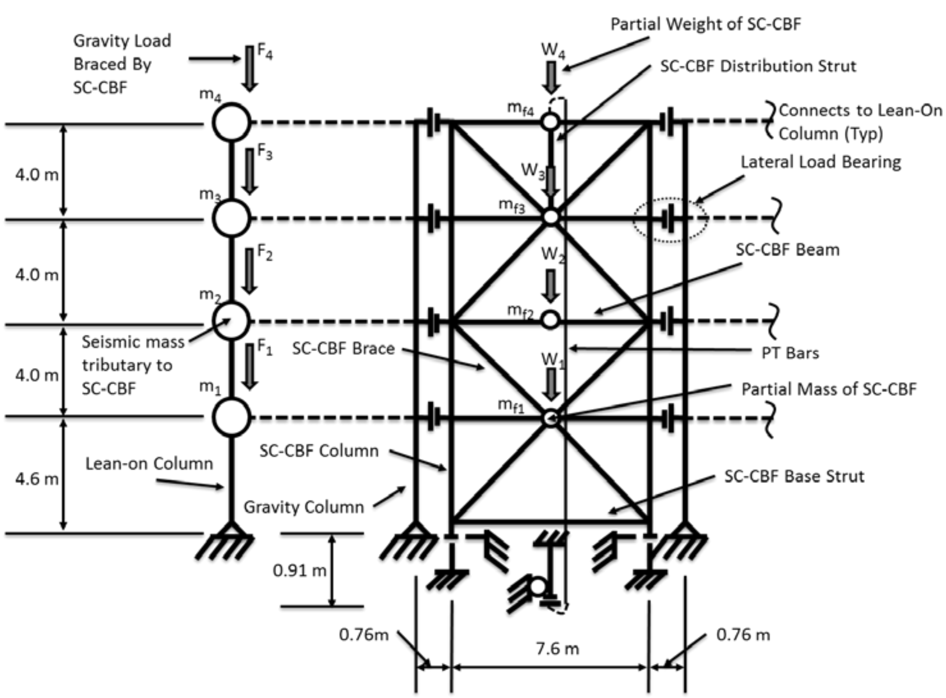

Fig. 6 – Schematic of numerical model layout for archetype SC-CBFs [7]

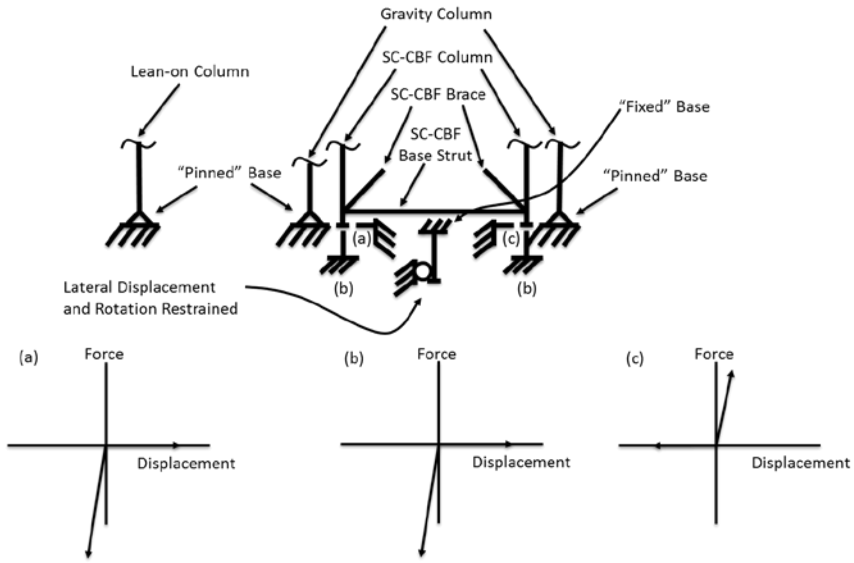

Fig. 7 – Numerical model boundary conditions for archetype SC-CBFs [7]

The adjacent gravity columns shown in Figure 6 are laterally constrained to the lean-on-column at each floor. The seismic floor mass is assigned to the horizontal degree of freedom at the lean-on column node. A small mass modeling the mass of the SC-CBF is applied to vertical and horizontal degrees-of-freedom of the center node of the SC-CBF at each floor.

Boundary conditions at the base of the SC-CBF are shown in Figure 7. The lean-on column and the gravity columns adjacent to the SC-CBF columns have pinned bases. A vertical and horizontal gap and contact condition is modeled at the base of each SC-CBF column by two zero-length elements. One zero-length element models the vertical gap and contact condition while the second models the horizontal gap and contact condition. The element connecting the zero-length element at the base of the PT bars to the foundation allows for only axial deformation.

Second order effects are considered and inherent damping is modeled using Rayleigh damping with 2.6% damping in the first mode and 6.1% in the third mode.

3.3 Ground Motion Ensemble

The ensemble of ground motions used to study the archetype SC-CBFs are shown in Figure 8 below. The ensemble is comprised of 18 scaled ground motion pairs (36 total ground motions) from the PEER-NGA database [14] selected and scaled to represent the design spectrum over a period range of 0.1-7.0 sec. These ground motions are recorded on sites with NEHRP Type D soil classification. The lowest usable frequency of each ground motion is 0.125 Hz or less, providing seismic input to periods of 8 sec or more. The ground motions are scaled so the geometric mean of the spectral acceleration for each ground motion pair matches the design spectrum over the period range of 0.1-7.0 sec (with a period increment of 0.01 sec) as shown in the Eq. (8). The scale factor for all ground motion pairs is less than 3.0.

$$SF_j = \frac{\sum_{k=1}^{n} SA_{TS}(T_k)}{\sum_{k=1}^{n} SA_{GM}(T_k)} \tag{8}$$

where,

SF_j is the scale factor for ground motion j in the ground motion set
T_k is the k^{th} period in a vector of n periods considered
$SA_{TS}(T_k)$ is the spectral acceleration of the target spectrum at period T_k
$SA_{GM}(T_k)$ is the spectral acceleration of the ground motion being scaled at period T_k.

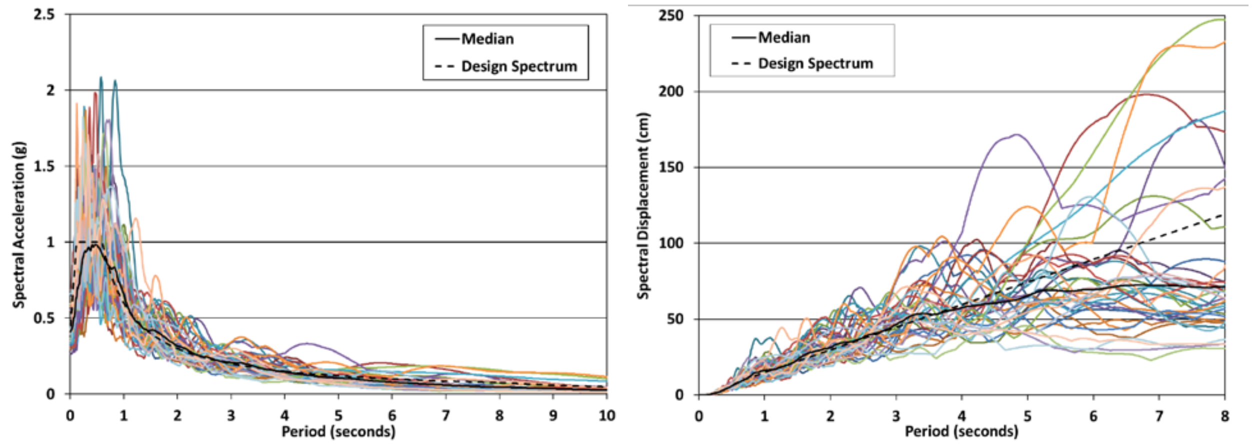

(a) (b)

Fig. 8 – Ground motion ensemble: (a) spectral acceleration, and (b) spectral displacement versus period [8]

3.4 Time-History Analyses Results and Validation of the Design Procedure

Figure 9(a) shows the peak roof drift demand for each time-history analysis and the median peak demand for all analyses. The median peak roof drift demand is less than 1.5% radians for all structures. The residual roof drift, shown in Figure 9(b), is negligible or zero. Therefore, these designs meet the previously stated objectives of the design procedure.

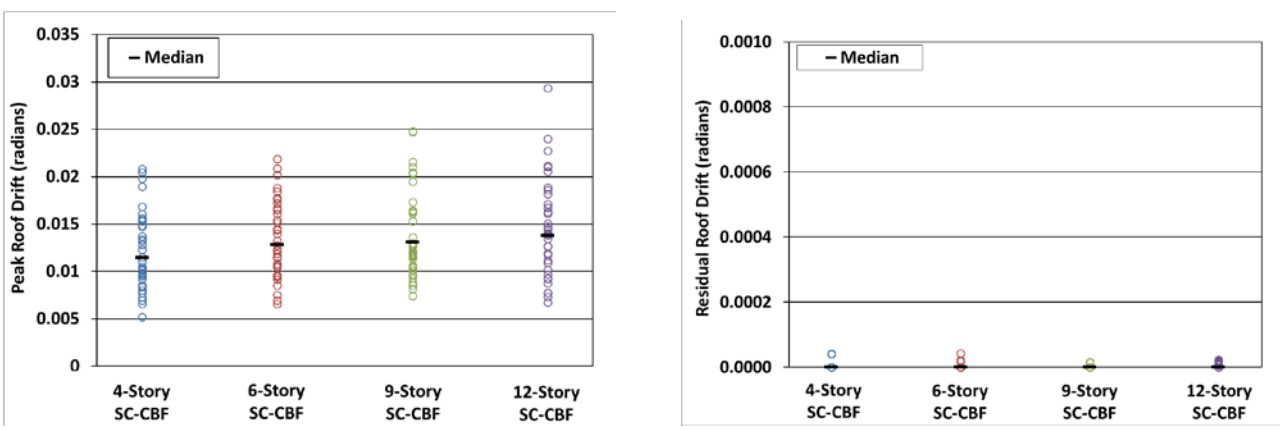

(a) (b)

Fig. 9 – Time-history analysis results: (a) peak roof drift demand and (b) residual roof drift [8]

Figures 10 and 11 show the normalized axial column utilization and normalized axial brace utilization, respectively, for the archetype SC-CBFs. The normalized axial column (or axial brace utilization) is the peak axial column force (or peak axial brace force) from the time history analysis divided by the factored (includes modal load factors) design demand. This ratio is an indication of how well the design procedure estimates the peak demand during the design basis earthquake. The design procedure intends to provide a low probability of member damage under the design basis earthquake. The design procedure achieves this objective since the 10% probability of exceedance (POE) value is less than 1.0 for all stories of all archetypes except the 10th story brace of the 12-story SC-CBF. In this case the 10% POE value is 1.03. However, it could be argued that the design results presented in Figure 10 and Figure 11 are too conservative. If a higher probability of member damage is acceptable to the designer, then the modal load factors (Eq. 1 and Eq. 2) may be reduced as described in [8].

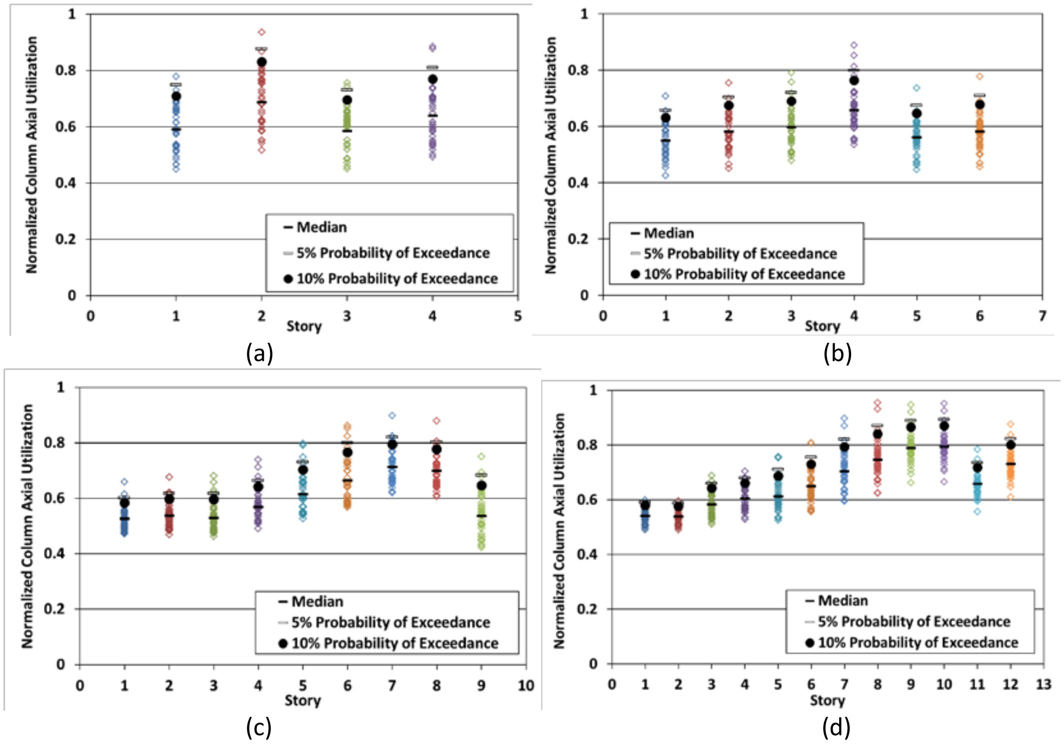

Fig. 10 – Normalized column axial utilization for (a) 4-story, (b) 6-story, (c) 9-story, and (d) 12-story [8]

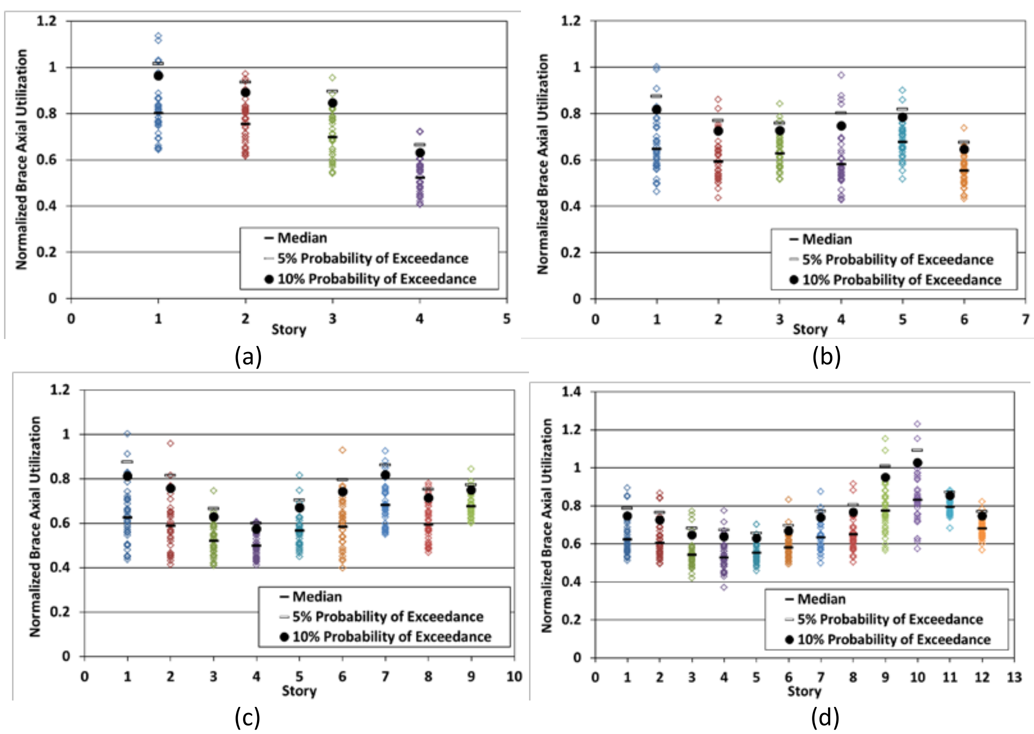

Fig. 11 – Normalized brace axial utilization for (a) 4-story, (b) 6-story, (c) 9-story, and (d) 12-story [8]

4. Summary and Conclusions

In this paper a seismic design procedure for steel SC-CBFs was presented and validated. This design procedure is based on the well-accepted response spectrum analysis procedure modified to account for specific SC-CBF behavior. This design approach ensures that the concepts can be easily understood and applied by practicing engineers. This modified design procedure does not uniformly reduce the spectral acceleration design spectrum, rather only reduces the first mode spectral acceleration to the value causing the overturning moment at yielding of the PT steel. The higher modes are increased using modal load factors so that a low probability of member damage under the design basis earthquake is achieved. The modal responses are combined using an adapted CQC procedure denoted 2CQC. In the 2CQC procedure the modal combination is carried out twice using different cross-modal correlation coefficients and the maximum result from these combinations is then used as the design demand. Special cross-modal correlation coefficients are used because a high correlation between modes often occurs at the time of peak member force demands.

The proposed design procedure was validated by studying four archetype SC-CBF structures of different heights. These archetype SC-CBF structures were each subjected to 18 ground motion pairs using nonlinear time-history analysis. The results of these analyses show that the proposed design procedure may be somewhat over conservative, but achieves the objective of a low probability of member damage under the DBE. The time-history analysis results also show that the median peak roof drift demand is not excessive (< 1.5% radians) and there is negligible residual drift.

5. References

[1] Roke, D., Sause R., Ricles J.M., Seo, C.-Y., and Lee, K.-S. (2006): Self-Centering Seismic-Resistant Steel Concentrically-Braced Frames. *Proceedings of the 8th U.S. National Conference on Earthquake Engineering*, San Francisco, California, USA.

[2] Roke D., Sause R., Ricles J.M., and Chancellor N.B. (2010): Damage-Free Seismic-Resistant Self-Centering Concentrically-Braced Frames. *ATLSS Report 10-09*, Lehigh University, Bethlehem, PA.

[3] Eatherton, M.R., Hajjar, J.F., Deierlein G.G., Krawinkler H., Billingon S., and Ma X. (2008): Controlled Rocking of Steel-Framed Buildings with Replaceable Energy-Dissipating Fuses. *Proceedings of the 14th World Conference on Earthquake Engineering*, Beijing, China.

[4] Chancellor N.B., Akbas G., Sause R. Ricles J.M., Tahmasebi E., and Joo A.L. (2012): Evaluation of performance-based design methodology for steel self-centering braced frame. *STESSA 2012, Proceedings of the 7th International Conference on Behavior of Steel Structures in Seismic Areas*, Santiago, Chile.

[5] Chancellor N.B., Roke D.A, Sause R., Ricles J.M., and Gonner N.P. (2011): Performance of Steel Self-Centering Braced Frame System During Intense Earthquake and Aftershock Ground Motions. *Proceedings of the 8th Conference on Urban Earthquake Engineering*, Tokyo, Japan.

[6] Gonner N., Chancellor N.B., Sause R., Ricles J.M., Roke, D., and Miranda J. (2010): Design, Experimental Setup, and Testing of Self-Centering Steel Concentrically-Braced Frame Test Structure. *ATLSS Report 10-06*, Lehigh University, Bethlehem, PA.

[7] Chancellor N.B., Sause R., Ricles J.M., Tahmasebi E., and Akbas T. (2013): Seismic Response of Post-Tensioned Steel Rocking Concentrically Braced Frames with Various Aspect Ratios. *COMPDYN 2013, Proceedings of the 4th ECCOMAS Thematic Conference on Computational Methods in Structural Dynamics and Earthquake Engineering*, Kos Island, Greece.

[8] Chancellor N.B. (2014): Seismic Design and Performance of Self-Centering Concentrically-Braced Frames. *Dissertation*, Lehigh University, Bethlehem, PA.

[9] Der Kiureghian A. (1981): A Response Spectrum Method for Random Vibration Analysis of MDF Systems. *Earthquake Engineering and Structural Dynamics*, 9, pp 419-435.

[10] AISC (2005): Seismic Provisions for Structural Steel Buildings. *American Institute of Steel Construction*, Chicago, IL.

[11] ASCE (2010): Minimum Design Loads for Buildings and Other Structures, ASCE7-10. *American Society of Civil Engineers (ASCE)*, Reston, VA.

[12] AISC (2005b): Steel Construction Manual, 13th Edition. *American Institute of Steel Construction*, Chicago, IL.

[13] Mazzoni S., McKenna F., Scott M.H., Fenves G.L., et al. (2009): Open System for Earthquake Engineering Simulation (OpenSEES) User Command-Language Manual. *Pacific Earthquake Engineering Research Center*, University of California, Berkeley.

[14] Pacific Earthquake Engineering Research Center (PEER) (2011): Ground motion database, http://peer.berkeley.edu/nga/earthquakes.html.